

Carboxy ester hydrolysis catalysed by a dinuclear, hexaazamacrocyclic zinc(II) complex. A model for zinc(II) aminopeptidases

Carsten Wendelstorf, Sabine Warzeska, Endre Kővári and Roland Krämer*

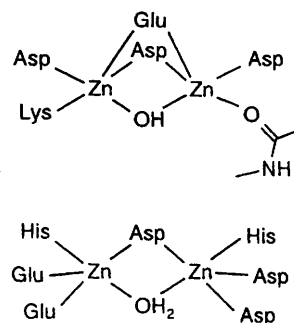
Anorganisch-Chemisches Institut der Universität, Wilhelm-Klemm-Strasse 8, D-48149 Münster, Germany

In order to investigate a mimic of aminopeptidase enzymes a novel macrocyclic dizinc complex was prepared. A protonated form of the dinucleating hexaazamacrocyclic L, $[H_4L][NO_3]_4 \cdot 2H_2O$, was characterized by X-ray crystallography. The macrocycle acts as a bis(tridentate) ligand in $[Zn_2L(NO_3)_4] \cdot 2H_2O$ **1**. Complex formation of L with Zn^{2+} in aqueous solution was investigated by potentiometric equilibrium measurements. Analysis of the titration data indicated that at $pH > 7$ the dinuclear, hydroxo-bridged species $[Zn_2L(\mu-OH)]^{3+}$ and $[Zn_2L(\mu-OH)(OH)]^{2+}$ dominate. Complex **1** is a catalyst for the hydrolysis of the activated carboxy ester *p*-nitrophenyl acetate, with no loss of activity for at least 2.7 catalytic cycles. The second-order rate constant for cleavage of *p*-nitrophenyl acetate by **1** at 20 °C and pH 8.65 is $(6.2 \pm 0.6) \times 10^{-3} \text{ dm}^3 \text{ mol}^{-1} \text{ s}^{-1}$. The pH dependence of the hydrolysis rate suggests that $[Zn_2L(\mu-OH)(OH)]^{2+}$ is the catalytically active species whereas $[Zn_2L(\mu-OH)]^{3+}$ displays little or no reactivity. The relevance of the investigations to dizinc active sites in aminopeptidases is discussed.

Aminopeptidases are widespread in nature and constitute an important subgroup of zinc-dependent proteases.¹ These enzymes catalyse the hydrolysis of the amino-terminal peptide bond in polypeptides. Whereas classical zinc proteases are mononuclear, aminopeptidases contain either one or two metal ions in the active site. The 'two-zinc' aminopeptidases represent, from a mechanistic point of view, a new class of metalloproteases. Recently, bovine lens leucine aminopeptidase (bLAP)^{2,3} and aminopeptidase from *Vibrio proteolytica* (AP)⁴ have been characterized crystallographically. Each zinc ion is fixed in the active site by ligation to four oxygen or nitrogen donor atoms of the protein (Scheme 1). A characteristic feature of both enzymes is the presence of a single bridging hydroxide (or water) coligand. Structural investigations on bLAP complexed with transition-state analogues strongly suggest a two-metal-ion mechanism.^{3,5} Bidentate co-ordination of the peptide substrate *via* the terminal amino group to Zn(1) and *via* the carbonyl oxygen to Zn(2), followed by nucleophilic attack of bridging hydroxide at the carbonyl C atom, was proposed.⁵ Related mechanisms involving a terminally bound OH^- nucleophile have also been considered.³ After removal of Zn the enzyme is reactivated by various other divalent metal ions, e.g. Co^{2+} , Mn^{2+} , Cu^{2+} and Mg^{2+} .

Co-operativity of two metal ions, in particular zinc(II), is also a widespread functional motif in enzymatic phosphate ester hydrolysis.⁶ Recent studies on hydrolytic cleavage of phosphate mono- and di-esters by dinuclear metal complexes have not only contributed to a better understanding of enzymatic two-metal mechanisms but have also resulted in the development of highly efficient synthetic reagents for the hydrolysis of activated phosphate esters and oligonucleotides.⁷ In contrast, hydrolysis of carboxy compounds by dinuclear metal complexes is much less well explored, although there is substantial interest in abiotic catalysts for the selective hydrolysis of polypeptides under mild conditions.⁸ Karlin and co-workers⁹ have recently reported rapid stoichiometric cleavage of dimethylformamide by a dinuclear copper(II) complex.

Dinuclear complexes of polyazamacrocyclic ligands are of considerable interest as bioinorganic models for the structure and reactivity of dinuclear sites in metalloenzymes.¹⁰ However, such compounds have not widely been used to mimic biorelevant hydrolysis reactions. Burrows and co-workers¹¹



Scheme 1 Structure of the the dinuclear zinc sites in bovine lens leucine aminopeptidase (left) and in aminopeptidase from *Vibrio proteolytica* (right)

have reported stoichiometric carboxy ester hydrolysis by a dinuclear nickel(II) macrocyclic complex which serves as a model for the dinickel(II) site in urease. Several macrocyclic dizinc compounds which are structurally related to dinuclear zinc sites in hydrolase enzymes have been described.¹²

To study the hydrolysis of carboxyl substrates by a dizinc complex we have synthesized $[Zn_2L(NO_3)_4]$ **1** where L is a dinucleating ligand containing two tridentate 2,6-bis-(aminomethyl)pyridine subunits. Tridentate chelation of Zn guarantees sufficient stability of the complex in aqueous solution. At the same time, free co-ordination sites remain at each metal ion for substrate binding and catalysis. Strict preorganization of the zinc ions by the relatively rigid macrocyclic framework facilitates incorporation of bridging OH^- . Potentiometric and 1H NMR studies suggest that the solution structure of **1** is related to the dizinc core in aminopeptidases by the presence of a single bridging OH^- at pH 7. Kinetic studies on the hydrolysis of the activated carboxylic ester *p*-nitrophenyl acetate by **1** are presented.

Results and Discussion

Syntheses

The preparation of the hexaaza macrocycle L has been described.¹³ Although L is available in analytically pure form,

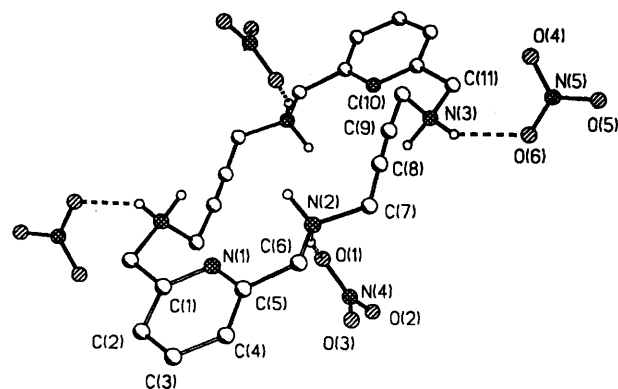
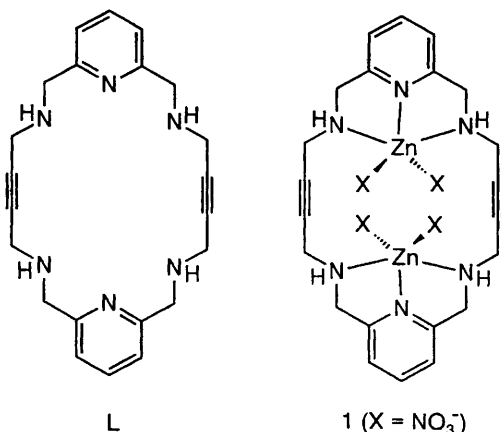


Fig. 1 Structure of $[\text{H}_4\text{L}][\text{NO}_3]_4 \cdot 2\text{H}_2\text{O}$ (water molecules not shown). The molecule is located on a crystallographic centre of symmetry. Hydrogen atoms were refined isotropically, but for clarity only the protons at N(2) and N(3) are included. Selected bond distances (Å): C(8)–C(9) 1.181(3), N(2)···O(1) 2.808, N(3)···O(6) 2.895

traces of impurities were detected in the ^1H NMR spectrum. To obtain a high-purity compound suitable for potentiometric titration studies (see below) we converted L into a crystalline ammonium salt, $[\text{H}_4\text{L}][\text{NO}_3]_4$, by treatment with HNO_3 in ethanol. Even with an excess of HNO_3 only the tetraprotonated compound is isolated. Recrystallization from methanol yields $[\text{H}_4\text{L}][\text{NO}_3]_4 \cdot 2\text{H}_2\text{O}$ which is free of any NMR impurities. The compound was characterized by ^1H NMR, microanalysis and X-ray crystallography. The dizinc complex $[\text{Zn}_2\text{L}(\text{NO}_3)_4]$ **1** was prepared in 77% yield from L and $\text{Zn}(\text{NO}_3)_2 \cdot 6\text{H}_2\text{O}$ in methanol. Attempts to grow X-ray quality crystals of **1** or of corresponding perchlorate and tetrafluoroborate complexes were unsuccessful. According to microanalytical data **1** is isolated as a dihydrate. Tridentate metal complexation by the 2,6-bis(aminomethyl)pyridine subunits is assumed, as observed in structurally characterized copper(II) complexes of L.¹³ The infrared NH band of **1** at $\tilde{\nu} = 3235\text{ cm}^{-1}$ lies in the typical range for Zn-co-ordinated secondary amine stretching frequencies¹⁴ (NH absorbance of free L: $\tilde{\nu} = 3347\text{ cm}^{-1}$). The co-ordination of zinc to the pyridyl groups is recognized by the shift of the pyridyl frequencies from 1593/1578 cm^{-1} for L to 1610/1587 cm^{-1} for **1**.¹⁵ Monodentate co-ordination of NO_3^- to the zinc ions in **1** is indicated by the N=O stretching frequencies at 1383 and 1298 cm^{-1} .¹⁶ Based on IR spectroscopic data we suggest for the zinc ions in **1** an N_3O_2 five-co-ordination which was established for dinitratozinc(II) complexes of tridentate aminopyridyl type ligands.^{15a} The ^1H NMR spectrum of **1** in D_2O at pD 7.0 displays signals for the aromatic (pyridine) and aliphatic ($\text{NC}_5\text{H}_3\text{CH}_2$, $\text{C}\equiv\text{CCH}_2$) protons at δ 7.79, 7.21 and 3.93, 3.49, respectively. Although the CH_2 protons of **1** are expected to be diastereotopic, $\text{NC}_5\text{H}_3\text{CH}_2$ and $\text{C}\equiv\text{CCH}_2$ give sharp singlets. This has also been observed for the zinc(II) complexes of related ligands¹⁴ and indicates rapid epimerization at the chiral nitrogen atoms.

Crystal structure of $[\text{H}_4\text{L}][\text{NO}_3]_4 \cdot 2\text{H}_2\text{O}$

X-Ray-quality crystals were obtained by slow diffusion of diethyl ether into a methanolic solution of $[\text{H}_4\text{L}][\text{NO}_3]_4 \cdot 2\text{H}_2\text{O}$. We have confirmed the molecular formula by crystal structure analysis since unambiguous knowledge of the composition of a compound is a prerequisite for the successful application to potentiometric equilibrium measurements. Furthermore, we were interested in the location of the protons in $[\text{H}_4\text{L}][\text{NO}_3]_4$ since only four of the potentially six sites are occupied.

Fig. 1 shows the structure of the $[\text{H}_4\text{L}][\text{NO}_3]_4 \cdot 2\text{H}_2\text{O}$ molecule which has a crystallographic centre of symmetry. The hydrogen atoms were located in the Fourier-difference map, and refined with variable U_{iso} . The four aliphatic nitrogen atoms are protonated whereas the less basic pyridyl nitrogens are not protonated. The ammonium protons at N(2) and N(3) form hydrogen bonds with nitrate counter ions.

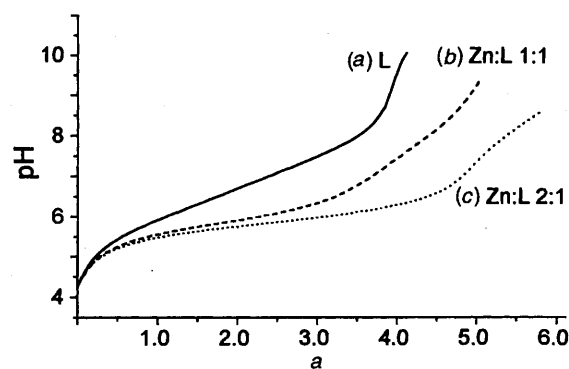
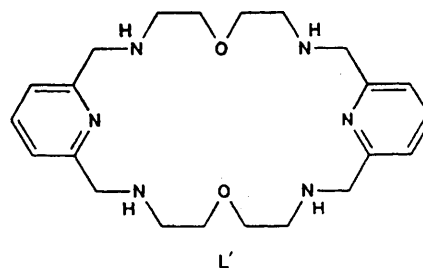


Fig. 2 Experimental pH titration curves (25 °C, $I = 0.100\text{ mol dm}^{-3}$) of solutions containing (a) 1.15 mmol dm^{-3} $[\text{H}_4\text{L}][\text{NO}_3]_4 \cdot 2\text{H}_2\text{O}$, (b) $0.880\text{ mmol dm}^{-3}$ $[\text{H}_4\text{L}][\text{NO}_3]_4 \cdot 2\text{H}_2\text{O}$ and $0.880\text{ mmol dm}^{-3}$ $\text{Zn}(\text{NO}_3)_2$ and (c) $0.714\text{ mmol dm}^{-3}$ $[\text{H}_4\text{L}][\text{NO}_3]_4 \cdot 2\text{H}_2\text{O}$ and $1.428\text{ mmol dm}^{-3}$ $\text{Zn}(\text{NO}_3)_2$; a corresponds to the molar equivalents of KOH added per mol L



Potentiometry

Potentiometric titrations (25 °C, water, $I = 0.1\text{ mol dm}^{-3}$ KNO_3) were performed to investigate complex formation of L with Zn^{2+} in H_2O . The pH titration curves for L alone and for 1:1 and 2:1 $\text{Zn}^{2+}:\text{L}$ ratios are given in Fig. 2. The stepwise acid-dissociation constants ($\log K$) of H_4L^{4+} are 5.51, 6.23, 7.00 and 7.74. In accordance with the crystallographic results we assume that the pyridyl nitrogens are not protonated above pH 2. This has also been reported for the related macrocycle L',¹⁷ the stepwise acid dissociation constants ($\log K$) of the tetraprotonated form being 8.75, 7.94, 7.36 and 6.79. The higher basicity of L' compared to L is explained by the electron-withdrawing effect of the alkyne groups in the latter compound.

Formation constants of the metal complex species present in $\text{Zn}^{2+}-\text{L}$ titration solutions are given in Table 1. For comparison the corresponding equilibrium constants of the $\text{Zn}^{2+}-\text{L}'$ system¹⁷ are included. Species distributions for 1:1 and 2:1 ($\text{Zn}^{2+}:\text{L}$) ratios are shown in Fig. 3. The complex-

Table 1 Protonation and equilibrium constants (log K values) for the complex formation of L with Zn^{2+} in H_2O at 25 °C, $I = 0.100 \text{ mol dm}^{-3}$ (KNO_3), calculated with BEST. Experimental (Fig. 2) and theoretical data were fitted with $\sigma_{pH} = 0.005$ for L alone (log K values in text), 0.0076 for the 1:1 Zn^{2+} :L system, and 0.0061 for the 2:1 Zn^{2+} :L system

Equilibrium	log K	
	L	L'
$[ZnL]/[L][Zn]$	5.86	8.89
$[Zn(HL)]/[ZnL][H]$	6.57	7.45
$[Zn(H_2L)]/[Zn(HL)][H]$	5.45	—
$[ZnL(OH)]/[H][ZnL]$	-8.36	-9.52
$[ZnL(OH)_2]/[H][ZnL(OH)]$	—	-11.00
$[Zn_2L]/[ZnL][Zn]$	2.88	3.80
$[Zn_2L(OH)]/[H][Zn_2L]$	-4.83	-7.07
$[Zn_2L(OH)_2]/[H][Zn_2L(OH)]$	-8.06	—

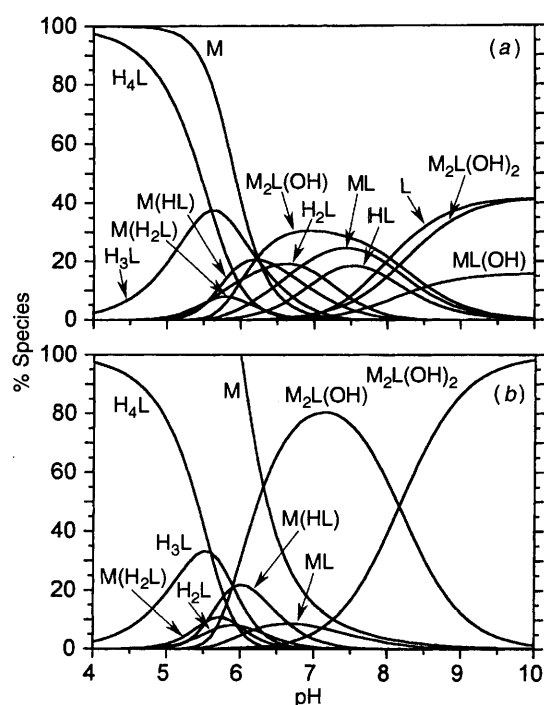


Fig. 3 The pH-dependent species distribution in solutions containing (a) L: Zn^{2+} in 1:1 molar ratio, (b) L: Zn^{2+} in 1:2 molar ratio, calculated from equilibrium data (Fig. 2) with the programs BEST and SPE. For clarity species with relative abundance < 5% were omitted

formation constants of L with the first and second equivalent Zn^{2+} are significantly lower than those of the more basic L'. Certain species are included either only in the L- Zn^{2+} system [$M(H_2L)$, $M_2L(OH)_2$], or only in the L'- Zn^{2+} system [$ML(OH)_2$]. However, $M(H_2L)$ and $M_2L(OH)_2$ have been detected by potentiometric studies of zinc(II) complex formation with 1,13-dioxo-4,7,10,16,19,22-hexaazacyclotetrasane¹⁸ or related ligands.^{12b,c,19} The pK_a value of co-ordinated water is 4.83 in $[Zn_2L(OH_2)_n]^{4+}$ and 7.07 in $[Zn_2L'(OH_2)_n]^{4+}$; 4.83 is much lower than the value expected for co-ordinated water in an independent [2,6-bis(aminomethyl)pyridine]zinc unit. For the first deprotonation of H_2O in aqua[2,6-bis(aminomethyl)pyridine]zinc $pK_a = 8.7$ has been detected.²⁰ Obviously, deprotonation of H_2O in $[Zn_2L(OH_2)_n]^{4+}$ is facilitated by formation of $[Zn_2L(\mu-OH)]^{3+}$ containing bridging hydroxide. Several azamacrocyclic dizinc complexes in which the metal ions are linked by a hydroxide ion have recently been characterized by X-ray crystallography.^{12a-c,21} The value $pK_a = 4.83$ for the dizinc complex of L is rather low compared to $pK_a > 7$ for the dizinc complexes of L'¹⁷ and related systems^{12b,c,19} but $pK_a < 5.3$

was reported for the equilibrium between the aqua and μ -hydroxo forms of a dizinc polyazamacrocyclic complex.²¹ In part the low pK_a of complex 1 might be attributed to the high degree of preorganization of the metal ions by the rigid macrocyclic framework of L. For the dicopper(II) complex of a closely related ligand we have detected an even lower $pK_a \approx 1.6$ for metal-bound water.²² A second water molecule in $[Zn_2L(OH_2)_n]^{4+}$ is deprotonated with $pK_a = 8.06$. Formation of the doubly hydroxide-bridged $[Zn_2(L(\mu-OH)_2)]^{2+}$ appears to be sterically impossible according to a ball-and-stick model. Thus, it should be $[Zn_2L(\mu-OH)(OH)]^{2+}$ containing one bridging and one non-bridging hydroxide.

In a solution containing 1 mmol dm^{-3} L and 2 mmol dm^{-3} Zn^{2+} the hydroxo complexes $[Zn_2L(\mu-OH)]^{3+}$ and $[Zn_2L(\mu-OH)(OH)]^{2+}$ are the dominant species at $pH > 7$ [Fig. 3(b)]. Interestingly, this is also valid for a 1 mmol dm^{-3} L-1 mmol dm^{-3} Zn^{2+} solution [Fig. 3(a)], although the contribution of other species including free L is more important in this case. Hydroxo bridging strongly favours the formation of dinuclear complexes. In solution $[Zn_2L(\mu-OH)]^{3+}$ mimics single μ -hydroxo bridging in the dizinc core of aminopeptidases.

To obtain additional information about the L- Zn^{2+} system in solution we have recorded 1H NMR spectra of complex 1 in D_2O at different pD values. Fig. 4 shows the spectra of a solution of 1 (8 mmol dm^{-3}) at pD 5.9, 6.3 and 7.0. At pD 5.9 two (or more) sets of signals both in the aliphatic and aromatic region of the spectrum indicate the presence of at least two different species, a major and a minor one [Fig. 4(a)]. On addition of 6 equivalents of $Zn(NO_3)_2$ at pH 5.9 the peaks are broadened but the relative abundance of the species does not change significantly. This observation rules out that the different signal sets are due to a di- and mono-nuclear complex since addition of an excess of Zn^{2+} should significantly reduce the concentration of the mononuclear complex. The concentration of the minor species decreases when the pD is raised to 6.3 by addition of NaOD [Fig. 4(b)]. At pH 7.0 the spectrum consists of a single set of signals [Fig. 4(c)]. A plausible explanation is the presence of Zn_2L and $Zn_2L(\mu-OH)$ which are in pH-dependent equilibrium and have different NMR spectra. With the approximation that these are the only species present in the NMR solutions, the pH-dependent $Zn_2L:Zn_2L(\mu-OH)$ ratio can be roughly estimated by integration, as 0.5 (pD 5.9), 0.1 (6.3) and ca. 0:1 (7.0). The same trend is reflected by the calculated ratios 0.09 (pH 5.9), 0.03 (6.3) and 0.01:1 (7.0), based on the potentiometrically determined $pK_a = 4.83$ of co-ordinated water in Zn_2L . The disagreement at pH 5.9 might be explained by the significant formation of mononuclear complexes which contribute to the NMR signals assigned to the 'minor species'. Formation of mononuclear complexes at pH 5.9 and 1 mmol dm^{-3} complex concentration is evident from Fig. 3(b), although dissociation of Zn_2L should be somewhat less favoured in the more concentrated NMR solutions. It was not possible to conduct the NMR experiment with an excess of Zn^{2+} to suppress formation of mononuclear species since zinc hydroxide precipitates at $pH > 6$.

Catalytic hydrolysis of *p*-nitrophenyl acetate

It is well known that simple zinc(II) complexes hydrolyse activated carboxy esters.²³ However, we are aware of only one study of Breslow and Singh²⁴ which focuses on ester hydrolysis by a dinuclear zinc complex. In this system the formation of an intramolecular hydroxo bridge is ruled out by the structure of the bis(macrocylic) ligand. To check the reactivity of 1 towards carboxylic substrates we have investigated hydrolytic cleavage of *p*-nitrophenyl acetate (npa).

Kinetic studies were undertaken in ethanol-water (1:1) since the solubility of npa is insufficient in pure water. Cleavage of npa is easily monitored by photometric detection of the released

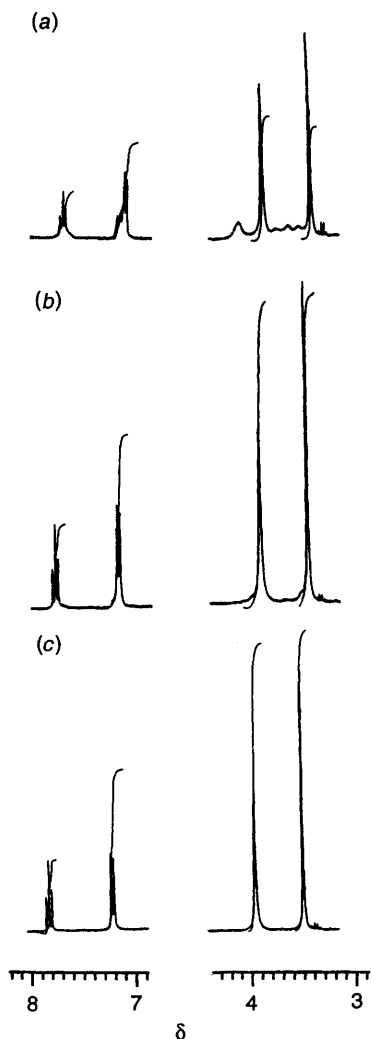


Fig. 4 Proton NMR spectra of a solution of complex **1** (8 mmol dm^{-3}) in D_2O at pD 5.9 (a), 6.4 (b) and 7.0 (c). The signals in (c) are attributed to $[\text{Zn}_2\text{L}(\mu\text{-OH})]^{3+}$ which is also the major species in (a) and (b). Smaller signals in (a) and (b) are attributed to $[\text{Zn}_2\text{L}]^{4+}$.

p-nitrophenolate. Fig. 5 shows the initial rate of npa hydrolysis by 5 mmol dm^{-3} **1** at varying substrate concentration at pH 8.65 and 20°C . For $[\text{npa}] = 0\text{--}30 \text{ mmol dm}^{-3}$ (30 mmol dm^{-3} is close to the solubility limit of npa) a linear increase in rate with substrate concentration is observed. This indicates second-order reaction of **1** and npa. Second-order behaviour is typical for npa hydrolysis by zinc(II) complexes.^{23a-c} The second-order rate constant, k_2 , for the hydrolysis of npa by **1** is $(6.2 \pm 0.6) \times 10^{-3} \text{ dm}^3 \text{ mol}^{-1} \text{ s}^{-1}$ at pH 8.65 and 20°C .

To demonstrate catalytic behaviour of the dizinc complex, hydrolysis of npa (20 mmol dm^{-3}) in the presence of **1** (5 mmol dm^{-3}) was monitored up to 75% substrate conversion at pH 8.65 (0.1 mol dm^{-3} ches) and 20°C . Under these conditions the decay of npa follows pseudo-first-order kinetics, with a rate constant $k_{\text{obs}} = (3.9 \pm 0.3) \times 10^{-4} \text{ s}^{-1}$. The pseudo-first-order rate constant for spontaneous hydrolysis of npa at pH 8.65 (0.1 mol dm^{-3} ches) and 20°C is $(0.8 \pm 0.1) \times 10^{-4} \text{ s}^{-1}$. Consequently, the first-order rate constant for npa hydrolysis catalysed by 5 mmol dm^{-3} **1** is $(3.1 \pm 0.3) \times 10^{-4} \text{ s}^{-1}$ at pH 8.65 and 20°C . Complex **1** is a perfect catalyst for at least 2.7 cycles. In contrast, only stoichiometric cleavage of npa by a dinickel(II) macrocyclic complex was reported by Burrows and co-workers.¹¹

The pH dependence of the hydrolysis reaction is of particular interest (Fig. 6). At pH 7.5 the reactivity of complex **1** is low but increases significantly at higher pH.

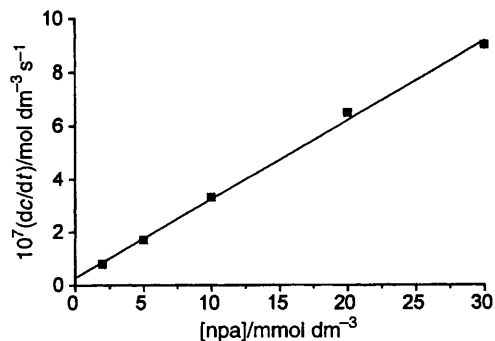


Fig. 5 Hydrolysis of *p*-nitrophenyl acetate (npa) by **1** (5 mmol dm^{-3}) in ethanol-water 1:1 (v/v) at pH 8.65 [buffer: 100 mmol dm^{-3} 2-(cyclohexylamino)ethane sulfonic acid (ches)] and 20°C . Dependence of the initial rate (dc/dt) of *p*-nitrophenolate release on npa concentration, corrected for spontaneous hydrolysis of npa. Data points are the average values from two kinetic runs, which were reproducible within 20%.

Although the kinetic experiments were performed in ethanol-water (1:1), the overall trends in the protonation behaviour of **1** should be roughly comparable with the findings of our potentiometric studies in water. Fig. 3(b) suggests that above pH 7 $[\text{Zn}_2\text{L}(\mu\text{-OH})]^{3+}$ and $[\text{Zn}_2\text{L}(\mu\text{-OH})(\text{OH})]^{2+}$ are the dominant species. Furthermore, for pH > 7.5 $[\text{Zn}_2\text{L}(\mu\text{-OH})(\text{OH})]^{2+}$ is the only species which increases in concentration with increasing pH {apart from a very small contribution of $[\text{ZnL}(\text{OH})]^{3+}$ }. The clear parallel between $[\text{Zn}_2\text{L}(\mu\text{-OH})(\text{OH})]^{2+}$ concentration and hydrolysis rate at pH 7.5–9.2 strongly suggests that the latter complex which contains a terminally bound hydroxide group is the hydrolytically active species (Scheme 2). The less nucleophilic bridging OH^- group in $[\text{Zn}_2\text{L}(\mu\text{-OH})]^{3+}$ appears to have little or no reactivity towards npa.

Nucleophilic attack of terminally co-ordinated hydroxide at the ester carbonyl group is a generally accepted mechanism of npa hydrolysis by mononuclear zinc complexes.²³ The second-order rate constants for npa hydrolysis by dinuclear **1** and by mononuclear azamacrocyclic zinc(II) complexes have the same order of magnitude.^{23b,c} Obviously, there is no efficient co-operativity between the two zinc ions of **1** in the hydrolysis of a simple carboxy ester. The presence of the second metal ion might become important when amino acid derivatives are utilized as substrates. Anchoring of the substrate at one zinc ion *via* the amino group should substantially increase the local concentration of the reactive carboxyl moiety and enhance the catalytic reactivity of **1**. In bovine lens leucine aminopeptidase, amino co-ordination of the peptide substrate supports fixation of the amide carbonyl group in close proximity to a co-ordinated OH^- nucleophile. Studies on the binding and hydrolysis of amino acid esters and amino acid amides by **1** are in progress. Investigations on the reactivity of the dicopper(II) complex of **L** will be presented elsewhere.

Experimental

The synthesis of macrocycle **L** has been described.¹³ Solutions for potentiometric titrations were prepared in ultrapure water saturated with dinitrogen. The exact Zn^{2+} concentration in a *ca.* 10 mmol dm^{-3} stock solution of $\text{Zn}(\text{NO}_3)_2 \cdot 6\text{H}_2\text{O}$ (reagent grade) was determined by titration with ethylenedinitrilotetraacetic acid. Solutions of $0.100 \text{ mol dm}^{-3}$ KOH (CO_2 free) and $0.100 \text{ mol dm}^{-3}$ HNO_3 were prepared from Dilute-it ampoules and standardized with potassium hydrogen phthalate. Potassium nitrate, the supporting electrolyte, was obtained in 99.5% purity. An NaOD stock solution for adjustment of pH in the ^1H NMR experiments was prepared by dissolving NaOH in D_2O .

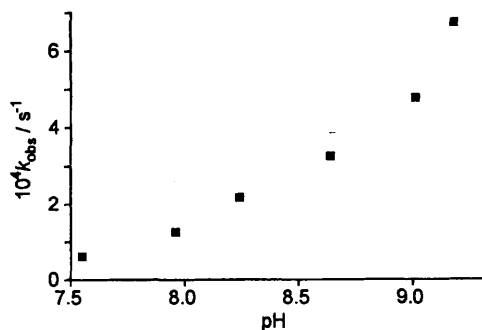
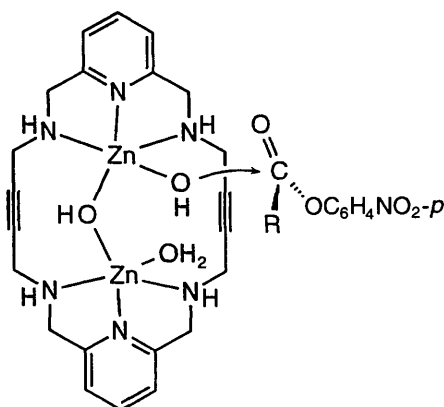


Fig. 6 Hydrolysis of *p*-nitrophenyl acetate (npa, 20 mmol dm⁻³) by complex **1** (5 mmol dm⁻³) in ethanol–water 1:1 (v/v) at 25 °C [buffer: 0.1 mol dm⁻³ tris(cyclohexylamino)methane (Tris) for pH < 8; 0.1 mol dm⁻³ ches for pH > 8]. Dependence of first-order rate constant (k_{obs}) on pH; k_{obs} was derived by the method of initial rates and is corrected for spontaneous hydrolysis of npa. Data points are the average values for two kinetic runs, which were reproducible within 20%



Scheme 2 Proposed mechanism for the hydrolysis of *p*-nitrophenyl acetate by $[\text{Zn}_2\text{L}(\mu\text{-OH})(\text{OH})]^{2+}$

Synthesis

$[\text{H}_4\text{L}][\text{NO}_3]_4 \cdot 2\text{H}_2\text{O}$. Macrocyclic L (100 mg, 0.27 mmol) was dissolved in ethanol–methanol (1:1, 10 cm³) and ethanol–concentrated HNO₃ (1:1, 2 cm³) was added dropwise with stirring. Addition of diethyl ether (30 cm³) with stirring yielded a white powder which was centrifuged off and washed twice with ethanol (2 cm³). Recrystallization from methanol afforded microcrystalline, white $[\text{H}_4\text{L}][\text{NO}_3]_4 \cdot 2\text{H}_2\text{O}$ (158 mg, 89%). ¹H NMR (D₂O, 300 MHz): δ 7.90 (t, 2 H, $J = 7.6$, pyridine H), 7.43 (d, 4 H, $J = 7.6$ Hz), 4.48 and 4.14 (s, 8 H each, NC₅H₃CH₂ and C≡CCH₂) (Found: C, 40.1; H, 5.30; N, 20.75. Calc. for C₂₂H₃₀N₁₀O₁₂·2H₂O: C, 39.9; H, 5.15; N, 21.15%).

$[\text{Zn}_2\text{L}(\text{NO}_3)_4] \cdot 2\text{H}_2\text{O}$ **1.** A solution of Zn(NO₃)₂·6H₂O (80 mg, 0.27 mmol) in methanol (2 cm³) was added dropwise with stirring to a solution of L (50 mg, 0.13 mmol) in methanol (2 cm³). Diethyl ether (20 cm³) was added with stirring. The white precipitate was centrifuged off, washed with diethyl ether (20 cm³) and vacuum-dried. Complex **1** was isolated as a dihydrate (81 mg, 77%). ¹H NMR (300 MHz, D₂O, pD 7.0 adjusted with NaOD): δ 7.79 (t, 2 H, pyridine H), 7.21 (d, 4 H, pyridine H), 3.93 and 3.49 (s, 8 H each, NC₅H₃CH₂ and C≡CCH₂) (Found: C, 33.9; H, 3.80; N, 17.1. Calc. for C₂₂H₂₆N₁₀O₁₂Zn₂·2H₂O: C, 33.5; H, 3.85; N, 17.75%).

Crystallography

X-Ray-quality crystals were grown by slow diffusion of diethyl ether into a solution containing $[\text{H}_4\text{L}][\text{NO}_3]_4 \cdot 2\text{H}_2\text{O}$ (10 mg) in methanol (5 cm³).

Crystal data. C₂₂H₃₄N₁₀O₁₄, $M = 662.6$, monoclinic, space group $P2_1/n$, $a = 12.770(3)$, $b = 9.303(2)$, $c = 12.958(3)$ Å, $\beta = 92.97(2)^\circ$, $U = 1537.3(6)$ Å³, $Z = 2$, $D_c = 1.431$ g cm⁻³, colourless columns, crystal dimensions 0.12 × 0.1 × 0.28 mm, $\mu(\text{Mo-K}\alpha) = 0.120$ mm⁻¹.

Data collection and processing. Siemens-P3 diffractometer, $T = 293(2)$ K, ω -2 θ scan mode, graphite-monochromated Mo-K α radiation ($\lambda = 0.71073$ Å); no absorption correction; 3506 reflections measured ($2.2 < \theta < 27.0^\circ$, $+h$, $+k$, $\pm l$), 3359 unique, 3359 observed with $I > 2\sigma(I)$; 276 parameters.

Structure analysis and refinement. Direct methods. Full-matrix least-squares refinement with all non-hydrogen atoms anisotropic. Hydrogens were located in the Fourier-difference map and refined isotropically. R (on F) and R' (on F^2) for $I > 2\sigma(I)$ were 0.047 and 0.104 where $R = \Sigma||F_o| - |F_c||/\Sigma|F_o|$, $R' = [\Sigma w(F_o^2 - F_c^2)^2/\Sigma(F_o^2)^2]^{1/2}$ and $w = 1/[\sigma(F_o^2) + (0.0597P)^2]$, where $P = [\max(F_o^2, 0) + 2F_c^2]/3$. Programs used are given in ref. 25.

Atomic coordinates, thermal parameters and bond lengths and angles have been deposited at the Cambridge Crystallographic Data Centre (CCDC). See Instructions for Authors, *J. Chem. Soc., Dalton Trans.*, 1996, Issue 1. Any request to the CCDC for this material should quote the full literature citation and the reference number 186/102.

Potentiometric measurements

Potentiometric titrations were carried out at 25 ± 0.2 °C with a Metrohm DMS-Titrino 716 instrument, fitted with a combined glass electrode. The titration cell was flushed with a slow stream of dinitrogen during the experiments. The electrode was calibrated by titration of HCl with KOH. Sample solutions were titrated with 0.100 mol dm⁻³ KOH, dispensed from a Metrohm 5 cm³ piston burette, with continuous magnetic stirring. For the titrations described here, 125 increments of KOH (40 μl) were added, with an equilibration time of 90 s after each addition. The ionic strength was adjusted to 0.100 mol dm⁻³ by adding appropriate amounts of KNO₃. The titration solution of L alone contained $[\text{H}_4\text{L}][\text{NO}_3]_4 \cdot 2\text{H}_2\text{O}$ (38.0 mg, 0.0573 mmol) in water (50 cm³). This solution was reemployed for the measurements of the 1:1 and 2:1 (Zn²⁺:L) systems by addition of appropriate amounts of the Zn(NO₃)₂ stock solution. At the end of each titration the amount of added KOH was neutralized by exactly the same quantity of 0.100 mol dm⁻³ HNO₃. The ionic strength was readjusted to 0.100 mol dm⁻³ by addition of KNO₃. Two measurements were performed for each system.

Calculation of equilibrium constants

Equilibrium constants given in Table 1 are concentration quotients and were calculated with the FORTRAN program BEST, using $\text{p}K_w = 13.78$.²⁶ The input for the program BEST consists of the components, their concentrations, initial estimates of the equilibrium constants for each species thought to be present in terms of these solution components, and the experimentally determined equilibrium data. The σ_{pH} values $\{ = [\Sigma w(\text{pH}_{\text{obs}} - \text{pH}_{\text{calc}})^2/\Sigma w]^{1/2}$, where $w = (\text{pH}_{i+1} - \text{pH}_{i-1})^{-2}$ are measures of the pH fit over the entire potentiometric equilibrium curve. Species distributions (Fig. 3) were calculated with the program SPE.²⁶

Hydrolysis of *p*-Nitrophenyl acetate (npa) by complex **1**

Hydrolyses of npa by 5 mmol dm⁻³ complex **1** at varying substrate concentrations (Fig. 5) were measured at 20 ± 0.5 °C by an initial-slope method following the increase in absorption at 400 nm of the released *p*-nitrophenolate with time. Appropriate amounts of stock solutions of **1** (in water), npa (in ethanol) and buffer (ches, $\text{p}K_a = 9.55$) were mixed in

ethanol-water (1:1, v/v, final ratio in the reaction solutions). The pH was adjusted to 8.65 by addition of NaOH or HNO₃, respectively. It was corrected according to literature recommendations²⁷ for ethanol-water (1:1) mixtures (pH = pH meter reading - 0.2). For the initial rate determination the following procedure was employed. In appropriate time intervals, aliquots (50 µl) of the reaction solution were added to water (2 cm³) (pH 7.00, buffer 10 mol dm⁻³ 3-morpholino propanesulfonic acid, pK_a = 7.2) and the absorbance at 400 nm was recorded immediately at 25 °C. Since at pH 7 yellow *p*-nitrophenolate and colourless *p*-nitrophenol are in pH-dependent equilibrium, the total concentration (*p*-nitrophenolate + *p*-nitrophenol) in these solutions was calculated using pK_a(*p*-nitrophenol, 25 °C) = 7.15²⁸ and ε₄₀₀(*p*-nitrophenolate) = 18 700 dm³ mol⁻¹ cm⁻¹. A linear increase of *p*-nitrophenolate concentration with time was observed in all cases (correlation coefficients > 0.997) when the conversion of npa was < 5%. All data were corrected for spontaneous hydrolysis of npa in the absence of **1**. A linear dependence of reaction rate (dc/dt) on npa concentration was found (Fig. 5, correlation coefficient 0.998).

The second-order rate constant for npa hydrolysis by **1** at pH 8.65 and 20 °C was calculated from $k_2 = dc(dr^{-1})/[npa]_0^{-1}[1]^{-1}$.

The pH dependence (Fig. 6) of the hydrolysis of npa (20 mmol dm⁻³) by complex **1** (5 mmol dm⁻³) at 20 °C was detected in the same fashion as described above. The buffers Tris, (pK_a = 8.3) and ches (0.1 mol dm⁻³) were used for pH < 8 and > 8, respectively. Hydrolysis at pH 8.28 was measured both in the presence of Tris and ches buffers. The rate was identical within the reproducibility of kinetic experiments. First-order rate constants were derived from the initial reaction rates (< 5% conversion of npa) which were corrected for the spontaneous hydrolysis of npa in the absence of **1**, $k_{obs} = dc(dr^{-1})[npa]_0^{-1}$.

To demonstrate catalytic turnover, the cleavage of npa (20 mmol dm⁻³) by **1** (5 mmol dm⁻³) was monitored to ca. 75% completion at pH 8.65 (0.1 mol dm⁻³ ches) and 20 °C. The decay of npa was a clean first-order reaction [linear dependence of ln(c/c₀) on t, correlation coefficient 0.998] with a rate constant $k = 3.9 \times 10^{-4} \text{ s}^{-1}$. The first-order rate constant for npa cleavage catalysed by **1**, $k = 3.1 \times 10^{-4} \text{ s}^{-1}$, was obtained by correction for the spontaneous hydrolysis of npa under the same conditions (first-order rate constant, $k = 0.8 \times 10^{-4} \text{ s}^{-1}$). This corresponds to a hydrolysis of 13.4 mmol dm⁻³ npa by **1** alone when the overall conversion of initially present npa (20 mmol dm⁻³) is 75%.

All kinetic experiments were run in duplicate, the reproducibility being within 20%.

Acknowledgements

This work was supported by the Deutsche Forschungsgemeinschaft and the Fonds der Chemischen Industrie. We thank M. Läge for the crystallographic data collection.

References

- 1 A. Taylor, *Trends Biochem. Sci.*, 1993, **18**, 167; *FASEB J.* 1993, **7**, 290; B. L. Vallee and D. S. Auld, *Acc. Chem. Res.* 1993, **26**, 543.

- 2 S. K. Burley, P. R. David, A. Taylor and W. N. Lipscomb, *Proc. Natl. Acad. Sci. USA*, 1990, **87**, 6878; S. K. Burley, P. R. David, R. M. Sweet, A. Taylor and W. N. Lipscomb, *J. Mol. Biol.*, 1992, **224**, 113.
- 3 N. Sträter and W. N. Lipscomb, *Biochemistry*, 1995, **34**, 14792.
- 4 B. Chevrier, C. Schalk, H. D'Orchymont, J.-M. Rondeau, D. Moras and C. Tarnus, *Structure*, 1994, **2**, 283.
- 5 N. Sträter and W. N. Lipscomb, *Biochemistry*, 1995, **34**, 9200.
- 6 E. E. Kim and H. W. Wyckoff, *J. Mol. Biol.*, 1991, **218**, 449; L. S. Beese and T. A. Steitz, *EMBO J.*, 1991, **10**, 25; A. Volbeda, A. Lahm, F. Sakiyama and D. Suck, *EMBO J.*, 1991, **10**, 1607.
- 7 M. Yashiro, A. Ishikubo and M. Komiyama, *J. Chem. Soc., Chem. Commun.*, 1995, 1793; D. Wahnou, A.-M. Lebus and J. Chin, *Angew. Chem.*, 1995, **107**, 2594.
- 8 M. Yashiro, T. Takarada, S. Miyama and M. Komiyama, *J. Chem. Soc., Chem. Commun.* 1994, 1757; E. L. Hegg and J. N. Burstyn, *J. Am. Chem. Soc.*, 1995, **117**, 7015.
- 9 N. N. Murthy, M. Mahroof-Tahir and K. D. Karlin, *J. Am. Chem. Soc.*, 1993, **115**, 10404.
- 10 P. K. Coughlin, J. C. Dewan, S. J. Lippard, E.-I. Watanabe and J.-M. Lehn, *J. Am. Chem. Soc.*, 1979, **101**, 265; M. G. Burnett, V. McKee and S. M. Nelson, *J. Chem. Soc., Chem. Commun.*, 1980, 829.
- 11 A. Salata, M.-T. Youinou and C. J. Burrows, *Inorg. Chem.*, 1991, **30**, 3454.
- 12 (a) C. Bazzicalupi, A. Bencini, A. Bianchi, V. Fusi, P. Paoletti and B. Valtancoli, *J. Chem. Soc., Chem. Commun.*, 1994, 881; (b) C. Bazzicalupi, A. Bencini, A. Bianchi, V. Fusi, L. Mazzanti, P. Paoletti, G. Piccardi and B. Valtancoli, *Inorg. Chem.*, 1995, **34**, 3003; (c) C. Bazzicalupi, A. Bencini, A. Bianchi, V. Fusi, P. Paoletti, G. Piccardi and B. Valtancoli, *Inorg. Chem.*, 1995, **34**, 5622; (d) H. Adams, N. A. Bailey, P. Bertrand, R. de Barbarin, O. Cecilia, D. E. Fenton, and S. Gou, *J. Chem. Soc., Dalton Trans.*, 1995, 275.
- 13 S. Warzeska and R. Krämer, *Chem. Ber.*, 1995, **128**, 115.
- 14 C. J. McKenzie, H. Toftlund, M. Pietraszkiewicz, Zb. Stojek and K. Slowinski, *Inorg. Chim. Acta*, 1993, **210**, 143.
- 15 (a) J. Wirbser and H. Vahrenkamp, *Z. Naturforsch., Teil B*, 1992, **47**, 962; (b) C. H. Kline and J. Turkevich, *J. Chem. Phys.*, 1944, **12**, 300.
- 16 N. F. Curtius and Y. Curtius, *Inorg. Chem.*, 1965, **6**, 804.
- 17 M. G. Basallote and A. E. Martell, *Inorg. Chem.*, 1988, **27**, 4219.
- 18 R. J. Motekaitis, A. E. Martell, J.-P. Lecomte and J.-M. Lehn, *Inorg. Chem.*, 1983, **22**, 609.
- 19 A. Bencini, A. Bianchi, P. Dapporto, E. Garcia-Espana, M. Micheloni and P. Paoletti, *Inorg. Chem.*, 1989, **28**, 1188.
- 20 I. O. Kady, B. Tan, Z. Ho and T. Scarborough, *J. Chem. Soc., Chem. Commun.*, 1995, 1137.
- 21 L. H. Tan, M. R. Taylor, K. P. Wainwright and P. A. Duckworth, *J. Chem. Soc., Dalton Trans.*, 1993, 2921.
- 22 S. Warzeska and R. Krämer, *Chem. Commun.*, 1996, 499.
- 23 (a) J. Chin and X. Zou, *J. Am. Chem. Soc.*, 1984, **106**, 3687; (b) E. Kimura, T. Shiota, T. Koike, M. Shiro and M. Kodama, *J. Am. Chem. Soc.*, 1990, **112**, 5805; (c) E. Kimura, I. Nakamura, T. Koike, M. Shionoya, M. Kodama, T. Ikeda and M. Shiro, *J. Am. Chem. Soc.*, 1994, **116**, 6764; (d) M. Ruf, K. Weis and H. Vahrenkamp, *J. Chem. Soc., Chem. Commun.*, 1994, 135.
- 24 R. Breslow and S. Singh, *Bioorg. Chem.*, 1988, **16**, 408.
- 25 G. M. Sheldrick, SHELXS 86, Program for Crystal Structure Solution, Universität Göttingen, 1986; SHELXL 93, Program for the Refinement of Crystal Structures, Universität Göttingen, 1993.
- 26 A. E. Martell and R. J. Motekaitis, *Determination and use of stability constants*, 2nd edn., VCH, New York, 1992.
- 27 R. G. Bates, *Determination of pH*, 2nd edn., Wiley, New York, 1964, p. 41.
- 28 M. M. Fickling, A. Fischer, B. R. Mann, J. Packer and J. Vaughan, *J. Am. Chem. Soc.* 1959, **81**, 4226.

Received 15th February 1996; Paper 6/01124A